Seed Science Research (2009) **19**, 225–239 doi:10.1017/S0960258509990122

Predicting seed dormancy loss and germination timing for *Bromus tectorum* in a semi-arid environment using hydrothermal time models

Susan E. Meyer[1]* and Phil S. Allen[2]

[1]US Forest Service, Rocky Mountain Research Station, Shrub Sciences Laboratory, Provo, Utah, USA; [2]Department of Plant and Wildlife Sciences, Brigham Young University, Provo, Utah, USA

(Received 8 February 2009; accepted after revision 15 July 2009)

Abstract

A principal goal of seed germination modelling for wild species is to predict germination timing under fluctuating field conditions. We coupled our previously developed hydrothermal time, thermal and hydrothermal afterripening time, and hydration–dehydration models for dormancy loss and germination with field seed zone temperature and water potential measurements from early summer through autumn to develop predictions of germination timing for *Bromus tectorum* at a semi-arid site in north-central Utah, USA. Model predictions were tested with a validation dataset based on concomitant seed retrieval experiments in 2 years. Predictions were generally in agreement with observed field germination time courses, even though integration across multiple precipitation events was necessary. Success of the modelling effort hinged on two factors. First, we used a soil capacitance sensor that measured seed zone (5 mm soil depth) water content accurately over a wide range. Second, simulations were built using physiologically based threshold models that can incorporate differences in germination timing for multiple germination fractions and for multiple stages of dormancy loss. Our results suggest that simulation models using hydrothermal time concepts can predict field germination phenology accurately. Seeds in this study integrated their experiences in a widely fluctuating environment in a manner consistent with the assumptions of hydrothermal time. Such threshold-based models also have the advantage of generality, as these concepts can be applied to many different species, environments and weather scenarios.

*Correspondence
Fax: +1 801-375-6968
Email: smeyer@fs.fed.us

Keywords: *Bromus tectorum*, capacitance sensor, dormancy loss, hydrothermal time, seed zone water potential, thermal afterripening time

Introduction

A primary objective of seed germination research, particularly with wild species, is to be able to predict when seeds will lose dormancy and therefore when they are likely to germinate in the field. Several empirically based models have been built with this objective in mind, and these models have met with varying degrees of success (e.g. Forcella, 1998; Kebreab and Murdoch, 1999; Vleeshouwers and Bouwmeester, 2001). An alternative to empirically based models is a methodology based on a more mechanistic understanding of how seeds lose dormancy and progress toward germination (Finch-Savage *et al.*, 2005; Allen *et al.*, 2007). The hydrothermal time model and its derived threshold models represent such a mechanistic or physiological approach. The threshold concept they embody has proven very useful for describing seed response at a population level to various stimuli that affect germination in the laboratory (e.g. Bradford, 1990; Ni and Bradford, 1992; Dutta and Bradford, 1994; Bradford *et al.*, 2007; Gianinetti and Cohn, 2007). Strict hydrothermal time models have not yet been used successfully for predicting germination phenology in the field. One obstacle to their use is the need for accurate quantification of seed zone water potential in order to create simulations that incorporate realistic microclimate data.

The concept of hydrothermal time (HTT) as it relates to seed germination was first introduced by Gummerson (1986) and was further developed by Bradford (1990, 1995). An extension of the more familiar concept of thermal time, the HTT model describes the process of seed germination in terms of

accumulation of progress toward radicle emergence. Germination rate varies as a function of both the seed population and its environment, namely the temperature and water potential of the germination medium. A seed population is characterized by its HTT requirement for germination and its base temperature, i.e. the threshold temperature below which germination is prevented; these are usually considered constants for the seed population as a whole. In contrast, the base water potential, i.e. the threshold water potential below which germination is prevented, is considered to be normally distributed within the population. Differences among fractions in germination rate are attributed to these differences in base water potential. Germination of a given fraction is prevented if temperature is below the base temperature or if water potential is below the base water potential for that fraction. Similarly, germination rate increases with temperature above the base temperature. Germination rate also increases with an increase in the distance between seed base water potential and ambient water potential.

The germination time for a particular fraction is related to its HTT parameters and to the temperature and water potential of its environment through the following equation:

$$\theta_{HT} = (\psi - \psi_{b(g)})(T - T_b)t_g \quad (1)$$

where θ_{HT} is the HTT requirement, i.e. the HTT accumulation necessary for radicle emergence to occur, ψ and T represent the water potential and temperature of the germination medium, T_b is the base temperature for germination, $\psi_{b(g)}$ is the base water potential for germination of fraction g, and t(g) is the time to germination for fraction g.

To extend the concept of HTT to a seed population, Gummerson (1986) used the probit transformation, which linearizes a normal distribution by expressing distances from the mean in terms of standard deviations. The following equation uses seed population-specific HTT parameters to predict time to germination for any fraction:

$$\text{Probit}\,(g/g_m) = [\psi - \psi_b(50) - \theta_{HT}/((T - T_b)t_g)]/\sigma_{\psi b} \quad (2)$$

where g/g_m is the fraction of viable seeds in the population, $\psi_b(50)$ is the mean (median) base water potential of the population, and $\sigma_{\psi b}$ is the standard deviation of base water potentials within the population. This equation can also be used to obtain estimates of HTT parameters for a seed population using data from germination time courses obtained at multiple temperatures and water potentials (Bradford, 1990, 1995).

The base water potential distribution for a seed population may vary as a function of time or environmental conditions. For example, one way to think of seed dormancy is to consider that dormant seeds have base water potentials above 0 MPa, the water potential of free water. As the seed population loses dormancy through time, its base water potential distribution shifts downward, so that an increasingly large fraction is able to germinate in free water. Also, the fractions capable of germinating slowly in water gain the ability to germinate more quickly as their base water potentials decrease during dormancy loss. Progressive acquisition of the ability to germinate in water, increasing germination rate in water, and increasing ability to germinate at more negative water potentials has been shown to take place in concert during dormancy loss in seeds of several species, including *Bromus tectorum* (Christensen *et al.*, 1996), *Elymus elymoides* (Meyer *et al.*, 2000), *Oryza sativa* (Gianinetti and Cohn, 2007) and others (Allen *et al.*, 2007).

The base water potential distribution of a seed population can also change as a function of temperature. As temperature increases above an optimum, germination rate and percentage decrease in much the same manner as if water potential were decreasing. This can be explained as an upward shift in the distribution of base water potentials at supra-optimal temperatures (Christensen *et al.*, 1996; Meyer *et al.*, 2000; Alvarado and Bradford, 2002).

The putative function of primary seed dormancy in the winter annual *B. tectorum* is to prevent precocious germination in response to summer rain events. The seeds lose dormancy through dry afterripening at summer temperatures and generally become non-dormant in time to germinate with autumn rains. The rate of dormancy loss (as measured by the downward shift in mean base water potential) is a linear function of temperature above a base afterripening temperature, as long as seed water potential remains above a threshold value of −150 MPa. We refer to a dormancy loss model that quantifies these relationships as a thermal afterripening time (TAR) model (Christensen *et al.*, 1996). Below −150 MPa, afterripening slows down as a linear function of decreasing water potential until it stops completely at a water potential around −400 MPa (Bair *et al.*, 2006). This has the effect of slowing afterripening when temperatures are very high, because such high temperatures are almost always associated with extremely dry conditions and very low seed water potentials. We refer to our model of the combined effects of temperature and water potential on dormancy loss rate as a hydrothermal afterripening time (HTAR) model.

Describing both dormancy loss and germination in terms of the same HTT parameters facilitates development of an integrated model that can link both processes through time. The coupled model should allow us to predict the status of a seed population at

the beginning of any rain event in the field and, based on the sequence of temperatures and water potentials experienced, predict which (if any) fractions will germinate in association with that rain event.

The experiments and simulations reported here represent an extension of studies that have already been published, and more details on experimental design can be found in these earlier papers (Christensen *et al.*, 1996; Bauer *et al.*, 1998; Bair *et al.*, 2006). The published papers reported on development of HTT models for *B. tectorum* seed collections made in 1994 and 1995 (Table 1) and on TAR and HTAR models for dormancy loss developed and field-validated for these seed collections (Table 2), but they stopped short of any effort to predict germination phenology in the field. Here we present our final synthesis of these datasets, to show how dormancy loss and hydrothermal time models can be integrated to predict germination timing under fluctuating field conditions.

Materials and methods

Hydrothermal time and dormancy loss models

In order to couple our published TAR and HTAR models for dormancy loss with hydrothermal time models for predicting germination phenology, some modifications to our previous efforts were necessary. During a rain event in the field, seeds may undergo rapid and sometimes extreme changes in temperature, and a model to simulate germination phenology under these conditions must be able to predict hydrothermal time accumulation across a wide range of temperatures. Because our earlier modelling efforts involved prediction and measurement of dormancy status through incubation of field-retrieved seeds under known conditions in the laboratory, we developed these models for single incubation temperature regimes (Bauer *et al.*, 1998). In order to use the models for field germination phenology simulations, a practical method for integrating dormancy status across incubation temperatures was required, i.e. a conceptual framework for estimating the mean base water potential at any temperature for any stage during dormancy loss. To achieve this, we first evaluated the necessary simplifying assumptions to determine how markedly they would affect the outcome of dormancy loss simulations. We then coupled our dormancy loss and germination models, executed and refined the simulations, and compared predicted germination time courses with germination time courses observed in the field.

The first step in our effort to devise a simple conceptual model for relating mean base water potential to incubation temperature at any stage of dormancy loss was to reanalyse the TAR data presented in Bauer *et al.* (1998) for four 1995 *B. tectorum* collections. When we tried this combined analysis for the original publication, analysis of covariance statistics indicated that seeds apparently afterripen at significantly different rates and even according to different base temperatures, depending on the incubation temperature. This led us to fit separate TAR regression equations for each incubation temperature, creating a serious obstacle to the development of a field germination phenology model.

Our approach here was to fit a TAR regression model integrated across incubation temperatures to these same data for each seed collection. We then used the combined model instead of the incubation-temperature-specific models to execute the same thermal afterripening simulations reported in Bauer *et al.* (1998). The base temperature for afterripening in

Table 1. Hydrothermal time parameters for six *Bromus tectorum* seed collections used in retrieval experiments at Point of the Mountain, Utah, in 1994 and 1995

	Hydrothermal time parameters						
				Recently harvested		Fully afterripened	
Seed population and year	θ_{HT} (MPa° days)	$\sigma_{\psi b}$ (MPa)	R^2	$\psi_b(50)$ 10/20°C (MPa)	$\psi_b(50)$ 20/30°C (MPa)	$\psi_b(50)$ 10/20°C (MPa)	$\psi_b(50)$ 20/30°C (MPa)
1994							
Whiterocks[a]	42	0.31	0.89	−0.15	−0.01	−1.22	−1.22
Hobblecreek[a]	37	0.31	0.91	−0.15	+0.04	−1.17	−1.17
1995							
Whiterocks[b]	43	0.60	0.90	−0.13	+0.50	−1.15	−1.15
Hobblecreek[b]	35	0.33	0.83	−0.12	+0.14	−1.20	−1.20
Potosi Pass[b]	22	0.36	0.82	+0.12	+0.84	−1.11	−0.81
Strawberry[b]	52	0.31	0.79	−0.81	−0.16	−1.27	−1.27

[a] From Bair *et al.* (2006).
[b] From Bauer *et al.* (1998).

Table 2. Thermal (TAR) and hydrothermal afterripening (HTAR) time parameters for two 1994 *B. tectorum* collections and TAR parameters for four 1995 *B. tectorum* collections used in field retrieval experiments

	TAR models					HTAR models[c]		
Seed population and year	T_L[d] (°C)	DLR[e] (MPa-°weeks^{-1})	R^2	N	P	Slope (°weeks^{-1})	Y intercept (MPa-°weeks^{-1})	X intercept[f] (MPa)
1994								
Whiterocks[a]	13	−0.0058	0.879	22	<0.0001	−0.0000241	−0.0091	−378
Hobble Creek[a]	13	−0.0052	0.787	24	<0.0001	−0.0000241	−0.0091	−378
1995								
Whiterocks[b]	7	−0.0063	0.871	41	<0.0001	–	–	–
Hobble Creek[b]	7	−0.0064	0.851	51	<0.0001	–	–	–
Potosi Pass[b]	13	−0.0053	0.889	55	<0.0001	–	–	–
Strawberry[b]	7	−0.0062	0.877	30	<0.0001	–	–	–

[a] From Bair *et al.* (2006).
[b] From Bauer *et al.* (1998).
[c] Hydrothermal afterripening time models were constructed only for the 1994 collections because simple thermal time models were adequate to predict field afterripening in 1995 (Bauer *et al.*, 1998).
[d] T_L = base temperature below which afterripening does not take place.
[e] DLR = dormancy loss rate, decrement in mean base water potential in MPa per unit of thermal time at water potentials = > −150 MPa.
[f] Base water potential below which afterripening does not take place. Data from storage at −150 MPa and −300 MPa were used in development of HTAR models for 1994, which quantify decrease in the DLR as a function of storage water potential below −150 MPa.

the combined model was determined using analysis of covariance, with incubation temperature as the class variable and thermal time as the continuous variable. Repeated analyses were conducted, changing the value of the base temperature until the best fit overall (R^2 value) was obtained. This simplified approach also differed from the earlier procedure in that a common slope was derived for the decrement in mean base water potential as a function of thermal time, with only the *y*-intercept or starting value changing as a function of incubation temperature. The common slope of decrease and common base afterripening temperature were then substituted into the field simulation, which used hourly temperature data from the field site in summer 1995 to drive the model for each seed population. We compared these new versions graphically with published models for each seed collection (Bauer *et al.*, 1998). We also extended these simplified afterripening models to predict dormancy status into the autumn. The earlier models had been terminated in late summer, when the first rains occurred and seeds began to accumulate hydrothermal time. The HTAR models for the 1994 collections that were used to execute the dormancy loss simulations in Bair *et al.* (2006) already included integration across incubation temperatures, so the only step needed for those models was to extend them into the autumn.

Another deficiency of the original dataset was that we evaluated seed germination across a relatively narrow range of incubation conditions. Based on measurements of field seed zone conditions, we realized that this would be a problem in germination phenology simulations. Therefore, about 6 months after the seeds were collected in 1995, we initiated a germination experiment with fully afterripened seeds that included a wider range of incubation temperatures, namely 10, 15, 20, 25, 30 and 40°C constant temperature, as well as a repeat of the alternating regimes used in the dormancy loss experiments (5/15, 10/20, 15/25 and 20/30°C 12 h:12 h). All tests were carried out for 28 d with a 12-h photoperiod as in the earlier tests and used the same protocols (Christensen *et al.*, 1996; Bauer *et al.*, 1998). These data were combined with data from earlier experiments to develop a set of equations relating mean base water potential to afterripening status and incubation temperature for each seed collection.

Field microclimate monitoring and seed retrieval experiments

As previously reported, seed retrieval and microclimate monitoring took place at the Point of the Mountain study site near Provo, Utah in 1994 and 1995. The plots were located at a big sagebrush/bluebunch wheatgrass site with sandy loam soil. Mean annual precipitation at this site is approximately 400 mm. Precipitation is concentrated in the winter and spring months, with only 15% falling in June, July and August. However, summer storms can be intense. The study was installed each year within a week of seed harvest in a randomized block design. Seeds were air-dried, placed inside nylon mesh bags, and buried approximately 5 mm below the soil surface (for details

see Bauer *et al.*, 1998; Bair *et al.*, 2006). Seeds were retrieved from the study site at weekly intervals, or sometimes more frequently during rain events in 1995, and field germination percentage was determined for four replications of 200 seeds for each seed collection on each date. These retrieval experiments were also the source of field validation data for the dormancy loss models reported in our earlier papers, obtained by incubating ungerminated seeds under controlled conditions.

Temperature and water potential of the seed zone (approximately 5 mm depth) at the field site were measured using thermistor sensors (Omnidata, Logan, Utah, USA) and soil capacitance sensors (Automata Inc., Grass Valley, California, USA), respectively. Measurements were recorded hourly, as an average of six readings at 10-min intervals, using a data logger (Omnidata Easylogger 900, Logan, Utah, USA). Soil capacitance varied as a function of water content and soil characteristics for the soil between the two flattened 64-cm prongs of the sensor. Laboratory external calibrations were performed with the Point of the Mountain field soil to determine water content values corresponding to soil capacitance readings; sensors were calibrated individually but showed little variation. Corresponding water potential values were determined using a soil water release curve for this soil (Hanks, 1992). We used the pressure plate method for the upper (wetter) part of the release curve (> -2 MPa) and equilibration over saturated salt solutions for the lower (drier) part (-2 to -400 MPa). The capacitance sensor with its calibration equations was able to produce meaningful water potential measurements over the entire range from 0 to -400 MPa. We also recorded air temperature, precipitation and relative humidity at the study site. The air temperature and relative humidity data were used along with the seed zone temperature data to develop an alternative method for estimating seed zone water potential in dry soils (-40 to -400 MPa) in 1994; these were generally in agreement with capacitance sensor water potential values over this range (Bair *et al.*, 2006).

Germination phenology models

We used Excel spreadsheet software (Microsoft Corporation, Redmond, Washington, USA) for execution of germination phenology simulation models. From field retrieval data, we knew which germination fractions had been observed for each seed collection and on which date. Our goal was to simulate germination times for multiple fractions, including those fractions that were actually observed to germinate in the field, so that we could compare graphically simulated and observed germination time courses.

The first step in developing the simulation model was to determine the mean temperature for each wetting event (defined as a precipitation event that resulted in seed zone wetting to > -4 MPa for at least an hour). These were the wetting events experienced by seeds between the time they were placed under field conditions and the time they achieved full germination.

We next needed to know the base water potential for each fraction of interest for a particular seed population at the beginning of each wetting event, so that simulated HTT could be accumulated according to that base water potential. First, we retrieved the value for accumulated thermal time at the initiation of each storm (wetting event) from our newly extended dormancy loss simulation for that seed population. This enabled calculation of the mean base water potential for each storm event using the relationships between mean base water potential, incubation temperature, and thermal afterripening time established in laboratory experiments (see results below). We then calculated base water potentials for the fractions of interest from the mean base water potential for that seed collection at that temperature for that point in time using the following equation, based on equation (2) above:

$$\psi_{b(g)} = \psi_b(50) + (\text{Probit}\,(g))(\sigma_{\psi b}) \quad (3)$$

This equation calculates the base water potential of any fraction from knowledge of the mean and standard deviation of the water potential distribution for a seed collection. According to our use of the hydrothermal time model, only the mean base water potential changes during dormancy loss; both the hydrothermal time requirement and the standard deviation of base water potentials are considered constants for the seed population (Christensen *et al.*, 1996).

Once the base water potential for a specific seed collection, germination fraction and storm of interest was determined, we could insert that value into equation (1), calculating HTT accumulated during each 1-hour time step, based on the seed zone temperature and water potential measured for that hour and the base temperature and base water potential for that fraction. We could then calculate the HTT accumulated during the course of the wetting period experienced during that storm for that fraction, sum HTT for that fraction across wetting periods, and determine at what point in real time the accumulated HTT was simulated to reach θ_{HT}, the HTT value required for radicle emergence. This procedure required a separate simulation for each germination fraction of interest, including modification of the mean base water potential for each storm where seed fractions are at a unique stage of dormancy loss and therefore have a unique base water potential.

We performed this series of simulations for each of the two 1994 and four 1995 seed collections included in the retrieval experiments.

Our first attempted simulations made two assumptions that we knew on theoretical grounds were probably false, so we were not surprised when these simulations sometimes predicted germination well in advance of observed field germination (data not shown). The first assumption was that the seeds would always sum progress toward germination across drying events. Frequently, summer storms were followed by rapid drying and long periods at very low water potentials. Our earlier research had shown that seeds 'remember' germination progress across wetting events only when these events are followed by gradual drying, cueing the seeds that subsurface water is present (Allen *et al.*, 1993, 1994; Debaene *et al.*, 1994). When seeds dry rapidly, they 'forget' the progress they have made, and must start over again when rehydrated. We therefore introduced the following limitation to HTT accumulation into the model. If the storm was followed by a drop in soil water potential from > -2 MPa to < -150 MPa within 24 h, we caused the seeds to 'forget' all the HTT accumulated to that point. If no such severe dehydration event occurred, we permitted the seeds to 'remember' their accumulated HTT.

The second assumption we had made was that the time necessary for physical imbibition at the beginning of every storm would 'count' toward the total HTT needed for radicle emergence, no matter how many times the seeds had to imbibe. In fact, relatively little physiological activity takes place in seeds during the first 6 h of imbibition (Bewley and Black, 1994). In experiments with continuously hydrated seeds, the HTT increment during imbibition is relatively small and is most simply included in the total HTT needed for germination. However, when the seeds must imbibe over and over again in a series of storms, the idea that more HTT accumulates during imbibition each time is not correct, and this error is multiplied with each storm. To compensate for this, we adjusted the models to 'count' only the 6-h imbibition period for the first 'remembered' storm. For each subsequent storm, HTT calculated to accumulate during the first 6 h, when seeds were primarily repeating physical imbibition, was subtracted from the total. The simulations we present here are based on models that include these two modifications.

For two of the six seed populations, simulation based on the above approach showed a relatively poor fit to observed field germination time courses. For heuristic purposes, we modified key parameters that were poorly quantified for these two seed populations and performed additional simulations using these modified parameters (explained in the final section of the Results).

Results

Hydrothermal time and dormancy loss models

When data from the 1995 storage experiments with four *B. tectorum* seed collections were fitted with TAR models integrated across incubation temperatures, the fit was nearly as good as for models developed for individual incubation temperatures (Table 2; Bauer *et al.*, 1998). At low temperature (10°C) the slope of change differed significantly from slopes of change at higher incubation temperatures (Bauer *et al.*, 1998). Including data from this temperature in the combined analysis flattened the common slope considerably (data not shown). We therefore dropped the 10°C data from the integrated TAR model, on the logic that imbibed seeds that are only partially afterripened rarely encounter such low temperatures in the field. We chose to sacrifice some accuracy in this rarely encountered part of the temperature range in exchange for increased accuracy at higher temperatures. We observed the poor fit of the combined slope at this lower temperature for three of the four seed populations. For the Mojave Desert population from Potosi Pass, Nevada, the slope at 10°C was similar to slopes at the higher temperatures. For the three higher temperatures included in the final analysis of covariance, the combined models accounted for 85–89% of the variance in the dependent variable mean base water potential and were all highly significant (Table 2). The common base afterripening temperature in these combined analyses was 7°C for each of the three northern Utah populations and 13°C for the Potosi Pass population.

When the published field simulations (Bauer *et al.*, 1998) were re-executed substituting the common base temperatures and slopes for the incubation temperature-specific parameters used in the earlier analysis, the simulations were generally remarkably insensitive to the changes (Fig. 1). The fit of the model to observed values improved slightly for the Potosi Pass simulations, whose parameters had been changed the most. The model fits were slightly worse for the Whiterocks simulations and were very similar to the earlier runs for the other two seed collections. We concluded there was sufficient support for the use of these integrated TAR models and their resulting simulations in our current germination phenology modelling effort.

In the experiment with multiple constant and alternating incubation temperatures for fully afterripened *B. tectorum* seeds collected in 1995, analysis of covariance showed that there were no significant differences in mean base water potential between constant and alternating temperatures for any collection. In addition, mean base water potential did not increase with increasing incubation temperature at temperatures below the optimum (slopes not

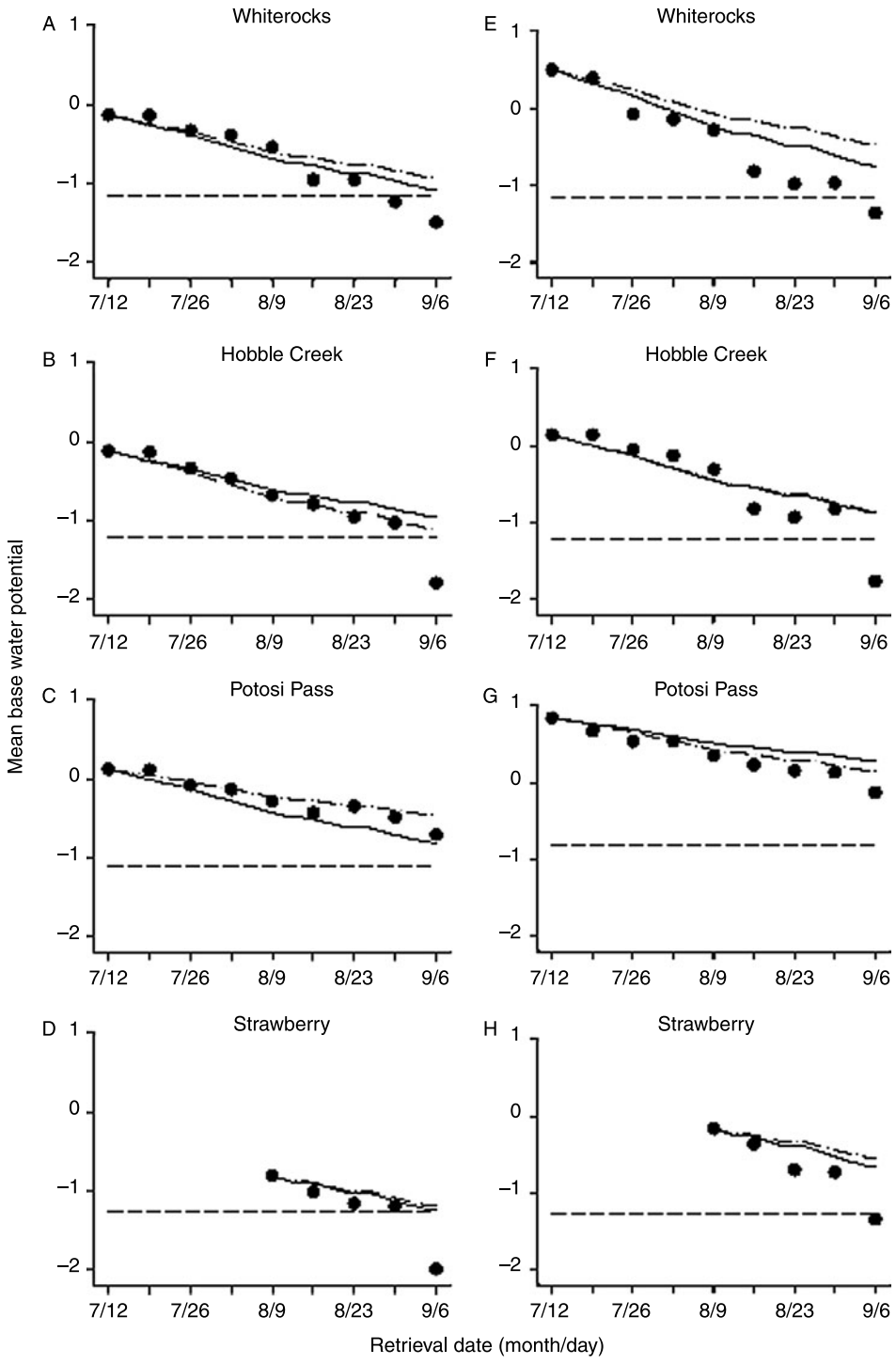

Figure 1. Field dormancy loss simulations for four 1995 *Bromus tectorum* collections based on unique thermal afterripening time parameters for each incubation temperature (solid lines, from Bauer *et al.*, 1998) and on thermal afterripening time parameters integrated across incubation temperatures (dot-dash lines, see Table 2) for each collection. Solid circles show validation data based on weekly retrieval of seeds from the field. (A)–(D) Post-retrieval incubation at 10/20°C; (E)–(H) post-retrieval incubation at 20/30°C. Horizontal dashed lines show mean base water potential of fully afterripened seeds for each seed collection and incubation temperature.

significantly different from zero; data not shown). This permitted us to model the sub-optimal part of the incubation temperature range as a line of slope zero for each collection. There was a clear increase in mean base water potential above 25°C for seeds from Whiterocks and Hobble Creek and above 20°C for seeds from Potosi Pass, but there was sufficient germination at 30°C to permit an estimate of the mean base water potential at this temperature. Seeds from Strawberry had the same mean base water potential at 30°C as at lower temperatures but, like the other three collections, were completely unable to germinate at 40°C. Based on our limited data in the supra-optimal range, we have proposed a model with a linear increase in mean base water potential as a function of temperature above the optimum (Fig. 2A–D).

We propose a parallel supra-optimal temperature model for recently harvested seeds (Fig. 2A–D). The range of mean base water potentials is shifted upward for recently harvested seeds relative to fully afterripened seeds, and the optimum temperature for recently harvested seeds is often lower. In practice, there was a trend for an increase in mean base water potential with incubation temperature even at temperatures shown as sub-optimal in these schematic graphs (data not shown), but because these sections of the graph had slopes that did not differ significantly from zero, they are also modelled as lines of slope zero. The slope of increase in mean base water potential with temperature in the supra-optimal range for recently harvested seeds is based largely on the mean base water potential for 25°C. These slopes generally resembled the slopes of increase in mean base water potential with temperature above the optimum based on 30°C for fully afterripened seeds. Although there were insufficient data for a formal test of equivalence, we have modelled these slopes as parallel for the sake of simplicity.

Combining relationships between mean base water potential and incubation temperature at different stages of afterripening shown in Fig. 2A–D with slopes of change in mean base water potential as a function of thermal time in Table 2 results in the relationships seen in Fig. 2E–H. Slopes of change through thermal afterripening time are constant across incubation temperatures for each collection, but different incubation temperatures have different initial and final mean base water potentials and therefore different thermal time periods necessary for seeds to become fully afterripened. According to our model, at the optimum temperature for recently harvested seeds and below, initial and final values of the mean base water potential for a seed population are constant, so that the lowest lines in Fig. 2E–H represent the change in value for all temperatures in the sub-optimal range.

The conceptual model for each 1995 collection (Fig. 2) permitted us to estimate a mean base water potential for any incubation temperature at any stage during afterripening (i.e. after the passage of any known amount of thermal afterripening time). This conceptual model was most strongly supported at temperatures below 30°C and for fully afterripened seeds, and should be considered provisional at supra-optimal temperatures. We used a similar procedure for 1994 collections, but we had to extrapolate from only two incubation temperatures, so that conceptual models for these collections required an additional assumption, namely that seeds collected from a given population have similar sub-optimal and supra-optimal temperature responses each year. This assumption may or may not be correct.

Field microclimate monitoring and seed retrieval experiments

Field seed zone temperature data generally confirmed decisions we made in earlier steps of model development. For example, summer temperatures never dropped as low as 10°C (Figs 3 and 4), confirming our decision to sacrifice some accuracy in this part of the temperature range for calculation of mean base water potentials during dormancy loss. By the time field temperatures dropped this low, seeds were generally fully afterripened in terms of their response at low incubation temperature. Similarly, our earlier decision to use 20/30°C as the laboratory temperature regime to imitate summer storms was confirmed by the fact that the mean seed zone temperature during a summer storm always fell between 22 and 25°C (Figs 3 and 4).

Precipitation patterns at Point of the Mountain in the 2 years of the study were similar, with a few small showers early in the summer, followed by fairly substantial August storms, and then a series of storms in early to mid-October (Figs 3 and 4). Total precipitation during this period was much higher in 1994 than in 1995, however. This resulted in much longer periods with water potentials in the range for HTT accumulation, especially in the fall. The patterns of change in seed zone water potential during and after storms were consistent across years. Especially during summer, the seeds spent very little time at intermediate water potentials. The soil would wet quickly to saturation following a storm and would dry just as abruptly to water contents too low for germination. This was because our sensors were located very near the surface, as seeds of these species would be, and insolation following storms dries this surface layer very quickly. The result was that, in terms of HTT accumulation, the seed zone was usually either wet, with a water potential very close to that of free

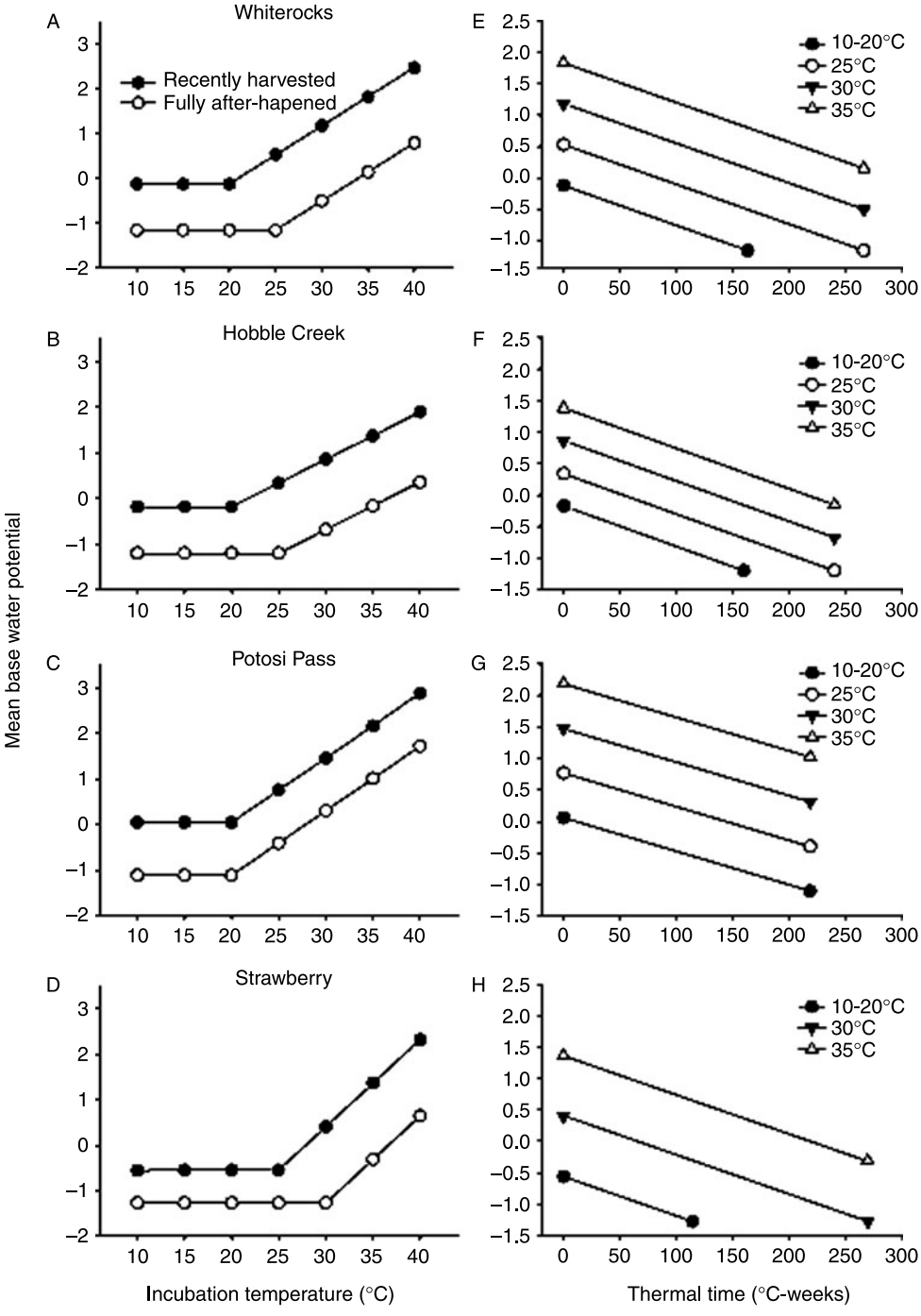

Figure 2. Schematic diagrams of the relationships between mean base water potential, afterripening status and incubation temperature for four 1995 *Bromus tectorum* seed collections, showing the relationship between $\psi_b(50)$ and incubation temperature for recently harvested and for fully afterripened seeds for (A) Whiterocks, (B) Hobble Creek, (C) Potosi Pass and (D) Strawberry, and showing dormancy loss [change of $\psi_b(50)$ from its initial to its final value] at each incubation temperature as a function of thermal time for (E) Whiterocks, (F) Hobble Creek, (G) Potosi Pass and (H) Strawberry. Initial and final $\psi_b(50)$ values change as a function of incubation temperature above the optimum but are constant at or below the optimum (indicated by less-than notation). See Table 2 for dormancy loss slopes; slope of increase in $\psi_b(50)$ as a function of temperature above the optimum is 0.136 MPa/degree for Whiterocks, 0.144 MPa/degree for Hobble Creek, 0.126 MPa/degree for Potosi Pass and 0.191 MPa/degree for Strawberry.

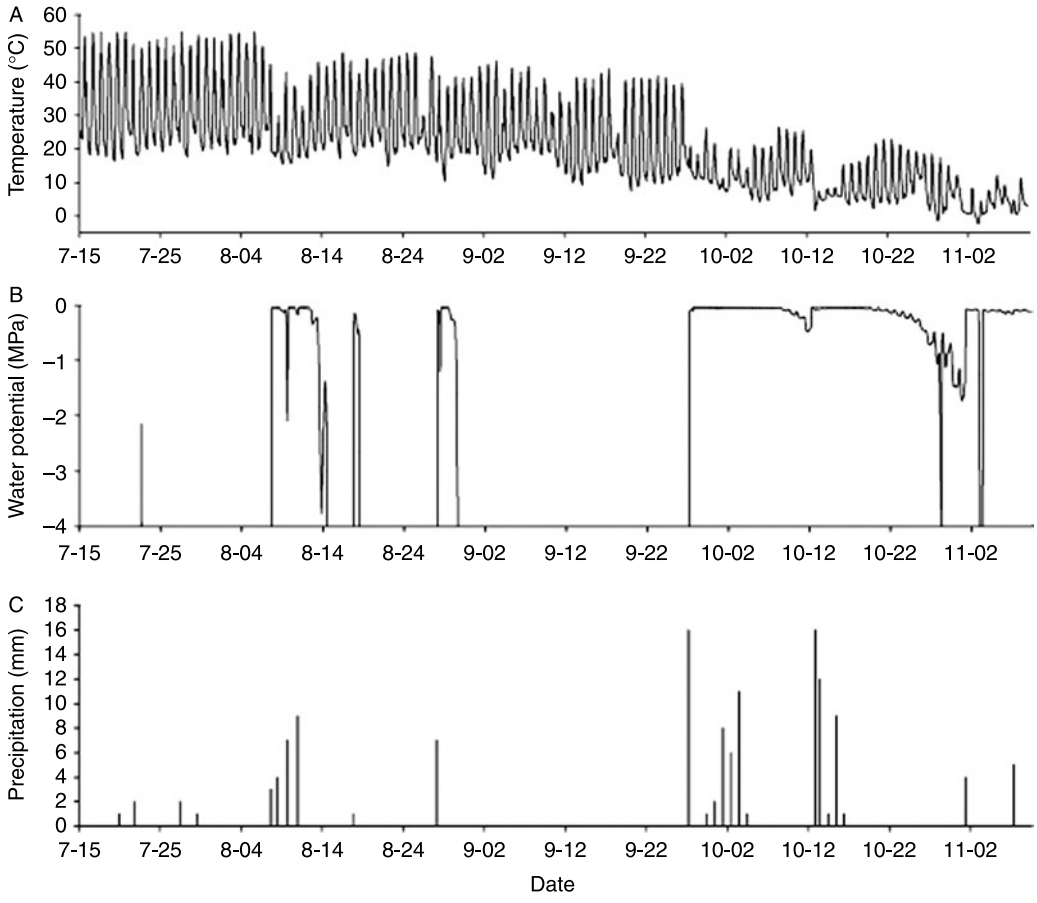

Figure 3. Field seed zone microclimate including (A) temperature and (B) water potential at 5 mm depth, and (C) precipitation data, recorded at the Point of the Mountain study site in summer and fall of 1994.

water, or too dry to support HTT accumulation. The exception occurred during late autumn storms, when temperatures were so low that even the soil surface dried slowly.

Results from the seed retrieval experiments mirrored the differences in summer precipitation patterns between the two study years. In 1995, no field germination occurred after summer storms, while in 1994 we observed some field germination. Seeds of all lots germinated to >95% during autumn storms both years, even though the absolute amount of rainfall received in autumn in 1995 was low (Figs 3 and 4). As mentioned earlier, low temperatures during these late storms kept the surface soil from drying and permitted germination in response to even relatively small precipitation events.

Another consequence of lower temperatures from late September onward was demonstrated by extending the afterripening simulations into the autumn. According to the simulations, afterripening slowed down dramatically after the middle of September, whether or not seeds had become completely non-dormant (data not shown). This was probably because of relatively high base temperatures for afterripening, and because seeds spent so much time at water potentials too high for afterripening to occur. Seeds germinated anyway in most cases, because they could accumulate the HTT needed for radicle emergence, but they apparently often failed to achieve the low mean base water potentials measured in laboratory germination experiments, particularly for higher incubation temperatures.

Germination phenology models

Our simulation models predicted germination time courses with reasonable accuracy within the limits of our field methodology in four of six cases (Fig. 5A–F). There are two things to note about the way these data are presented. First, seeds can only germinate when wet, and predictions that are only off by a few hours can 'push' a prediction a considerable distance forward or backward in real time, depending on the period between wetting events. Second, we only have the time of actual field germination recorded within

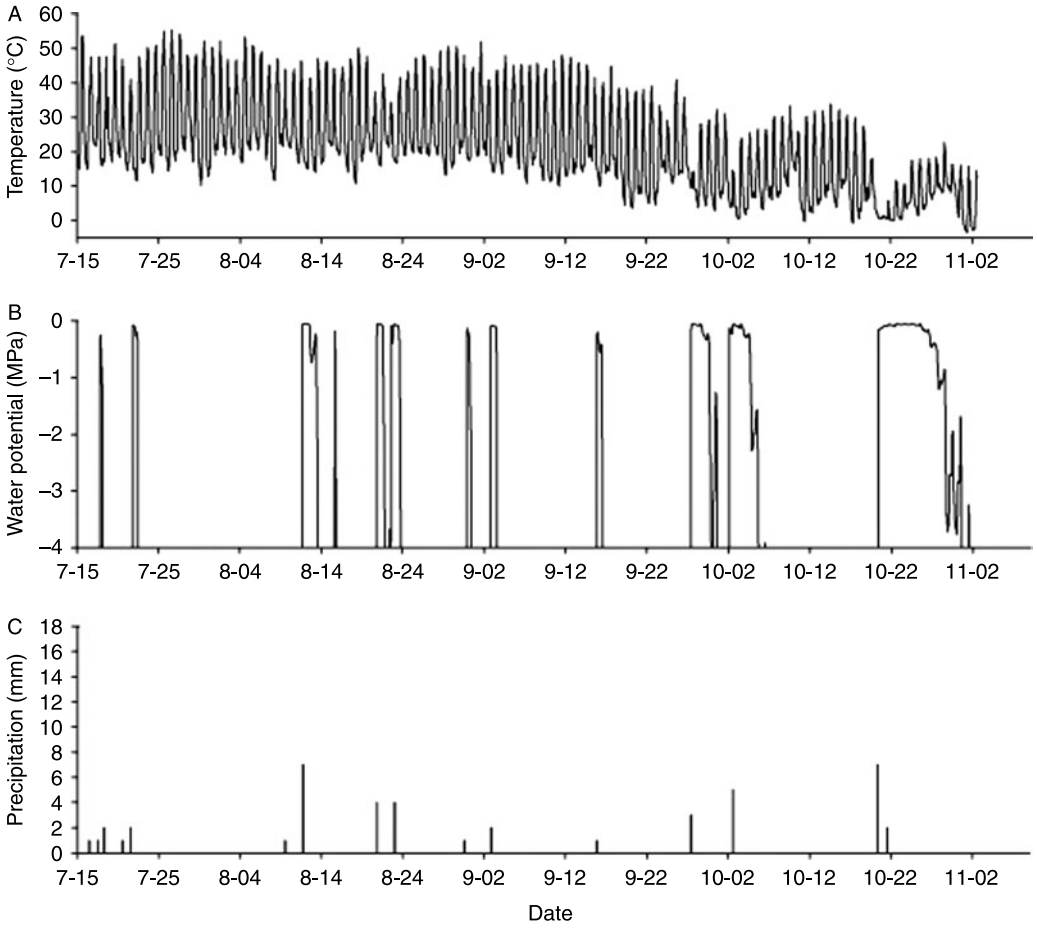

Figure 4. Field seed zone microclimate including (A) temperature and (B) water potential at 5 mm depth, and (C) precipitation data, recorded at the Point of the Mountain study site in summer and fall of 1995.

the level of precision provided by the intervals between retrievals. Predicted germination sometimes appears to be a few days ahead of observed germination during a storm, but this is often explained as an artefact of the retrieval interval. Overall, the germination time course predictions supported by theory were satisfyingly close to those that were actually observed.

Only one of four 1995 seed populations, Potosi Pass, failed to germinate substantially as predicted in our simulations (Fig. 5C). Because of its high base temperature for afterripening, the model for Potosi Pass predicted that even at the end of autumn, 27% of the seeds would have mean base water potentials too high to permit sufficient HTT accumulation for germination. In fact, complete germination of this seed population took place in late October. Potosi Pass did show delayed germination relative to the other 1995 seed populations, but once temperatures dropped to near-freezing in a late October storm (Fig. 4), the seeds germinated as if completely afterripened (Fig. 5C). This suggests that our extrapolation of the TAR model downward to these low imbibition temperatures was not accurate. By modifying the simulation to permit Potosi Pass seeds to reach the mean base water potential for fully afterripened seeds at sub-optimal temperature in time for this cold storm, we were able to produce a model with a much better fit (Fig. 5G). This modification resulted in a slightly worse fit for the earlier fractions, which germinated under warmer temperature conditions.

In 1994 we had fewer retrievals during rain events and therefore our resolution was not as good as in 1995 (Fig. 5E, F). We also had a weaker dataset upon which to base our model equations. However, these simulations successfully predicted germination in response to August storms, and also predicted germination in the correct storms in both summer and autumn for one of two cases, the Whiterocks 1994 seed population (Fig. 5E). For the Hobble Creek seed population, the model predicted germination to approximately 50% in response to summer storms, a pattern similar to that predicted (and observed) for the Whiterocks seed population (Fig. 5F). The reason for these similar predictions is evident from examination of HTT and HTAR parameters for the two seed populations, which

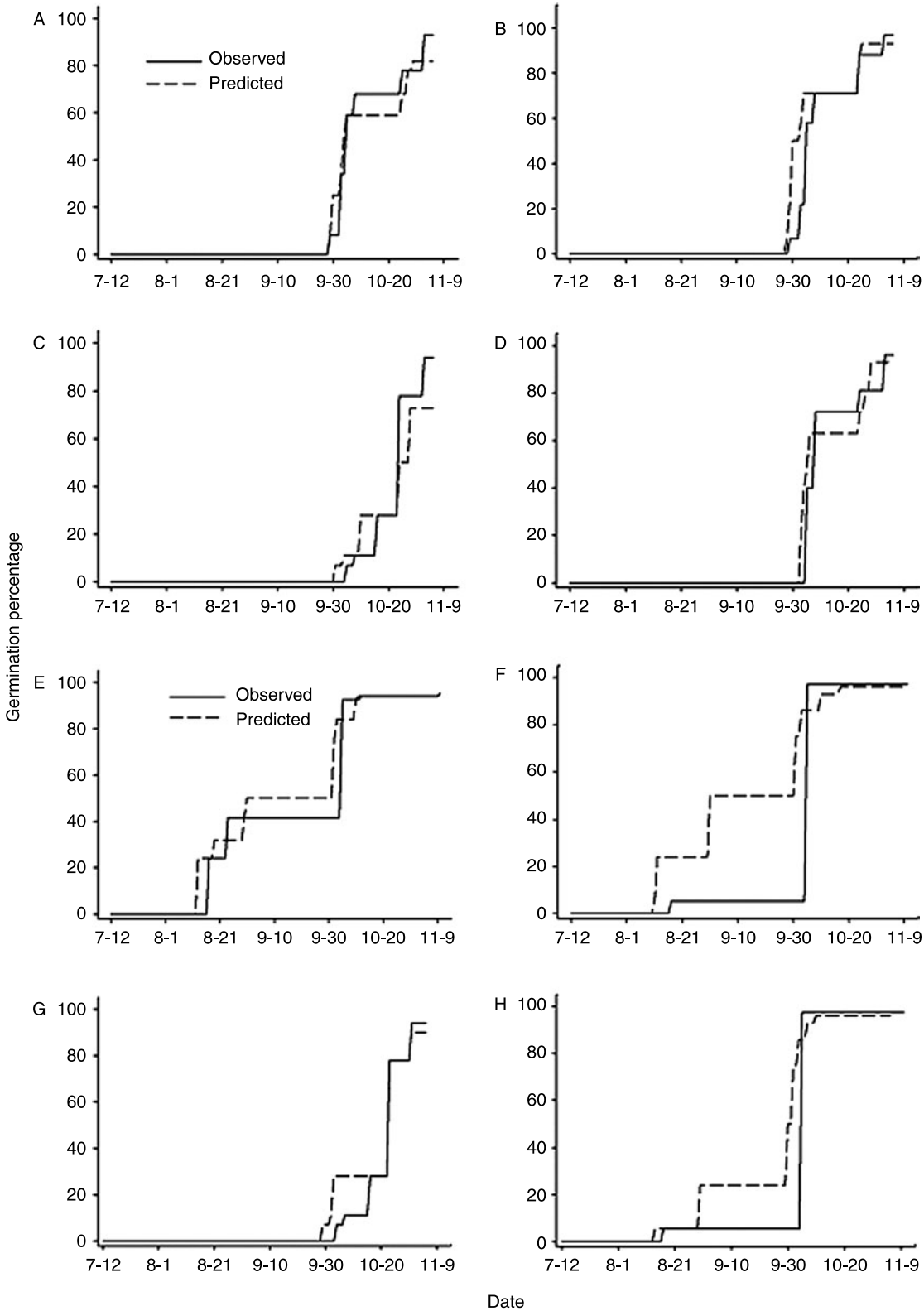

Figure 5. Simulated germination time courses for six *B. tectorum* seed collections included in retrieval experiments at Point of the Mountain, plotted against observed time courses from field seed retrievals: (A) Whiterocks 1995, (B) Hobble Creek 1995, (C) Potosi Pass 1995, (D) Strawberry 1995, (E) Whiterocks 1994, (F) Hobble Creek 1994, (G) Potosi Pass 1995 with modified model parameters, (H) Hobble Creek 1994 with modified model parameters.

are nearly identical (Tables 1 and 2). In fact, the Hobble Creek seed population only germinated to 8% in response to summer precipitation. We modified this simulation in two ways in order to improve model fit. We had no estimate of the slope of increase in mean base water potential above the optimum for the Hobble Creek 1994 seed population; we had provisionally used the value for the 1995 population in our original simulation. Our first modification was to double this slope. This resulted in a value similar to the slope estimated for the Strawberry collection in 1995, and had the effect of limiting HTT accumulation in early August storms, which had high mean temperatures (Fig. 4). Our second modification was to slightly decrease the value of $\sigma_{\psi b}$, the standard deviation of base water potentials for this population, from 0.31 to 0.25 MPa. This delayed germination of the early fractions and also improved the fit slightly for later fractions by moving their predicted germination times a few days earlier. But even with these modifications, the simulation still predicted 25% germination in response to August storms, when only 8% field germination was observed (Fig. 5H).

Discussion

The field seed zone in semi-arid environments is characterized by wide diurnal temperature fluctuations and intermittent moisture. In spite of the many challenges this presents for simulating field germination phenology, hydrothermal time models for dormancy loss and germination developed for *B. tectorum* in the laboratory were able to predict germination timing under fluctuating field conditions with a reasonable degree of accuracy. This was especially impressive in view of the fact that these models had to integrate HTT accumulation across multiple storms, many of which took place before seeds were fully afterripened. The way the model handled integration across storms was to sum HTT accumulation if the seeds dried slowly after a storm but not when they dried too quickly. This meant that HTT accumulated during small storms in summer 1995 was dropped, but not the HTT accumulated during the higher-rainfall storms of August 1994. These same late summer 1994 storms also resulted in some germination in the field. In more mesic environments and at greater depth, the seed zone is more likely to be continuously wet between storms, but in a semi-arid climate, the ability to correctly integrate HTT across storms is pivotal to successful predictions.

The fact that our model did not accurately predict summer germination for the Hobble Creek 1994 seed population may be due to an oversimplification of the effects of dehydration events in our model. We modelled the effect of rapid dehydration as uniform across all seed fractions, but in fact, our earlier studies showed that seed fractions on the brink of germination are more likely to be slowed down by rapid dehydration (Allen *et al.*, 1993; Debaene *et al.*, 1994). The effect in the field would be to slow down the early fractions, which have accumulated more HTT and are thus closer to germination, to a greater degree than later fractions that have accumulated little HTT. This could explain why the Hobble Creek 1994 seeds that were predicted to germinate in late August were slowed down and did not germinate until a later storm.

Accumulation of HTT across storm events could be considered seed priming, in that seeds germinate more quickly in a given wetting event because of past imbibition experience (Bradford and Haigh, 1994; Cheng and Bradford, 1999). Gianinetti and Cohn (2007) reported secondary dormancy induction in red rice when seeds were incubated at what would be considered priming potentials, i.e. potentials too low for radicle emergence. We did not observe or need to invoke either priming or secondary dormancy induction at intermediate water potentials in our model, probably because seeds spent little time at intermediate water potentials.

We made a number of simplifying assumptions in model development, and it is worth considering whether invoking more complex versions would have enhanced performance. For example, it has been amply demonstrated, both for *B. tectorum* (Christensen *et al.*, 1996; Bair *et al.*, 2006) and for red rice (Gianinetti and Cohn, 2007), that the decrease in mean base water potential through time during afterripening is not linear but negatively exponential. Gianinetti and Cohn (2007) provided an excellent discussion of the reasons for this non-linearity, and showed how a few transformations can make their more accurate and physiologically meaningful version of TAR tractable for linear analysis. We chose to stay with the simpler linear version because it fits almost as well over the range where seeds are afterripening quickly and because it was used in the development of our earlier dormancy loss models. The slower part of the afterripening process takes place after seeds are nearly fully afterripened. We showed that seeds may not even arrive at this part of the afterripening curve under field conditions before they germinate, so it is unlikely that using the curvilinear version of TAR would have improved simulation model performance.

We also made some simplifying assumptions about the relationships between mean base water potential and incubation temperature. For example, we modelled this relationship as a line of slope zero in the suboptimal range, extrapolated downward to 0°C, the base temperature for germination in this species. Similarly, the relationship between mean base water

potential and incubation temperature in the supra-optimal range is based on a relative paucity of data and could clearly benefit from refinement, although the positive linear relationship between mean base water potential and temperature above the optimum has been confirmed in other species (Rowse and Finch-Savage, 2003).

Another area where our model may be lacking is in measurement of changes in dormancy status at low temperatures. According to our TAR model, after-ripening stops below a base temperature, but we have unpublished data to suggest that the dormancy status of seeds can change at temperatures below the base, albeit slowly. We also lack solid data for how TAR impacts seeds at near-freezing incubation temperatures. The poor fit of our original simulation for the Potosi Pass seed population appeared to hinge on these problems. Permitting the seeds to accumulate HTT as if fully afterripened at near-freezing temperatures during late autumn storms, greatly improved model fit for this collection. In another experiment with a collection from the Potosi Pass population, we found that seeds incubated at near-freezing temperatures did not exhibit any primary dormancy even when recently harvested, in strong contrast to seeds incubated at temperatures at or above 10°C (Meyer and Allen, 1999). This supports the idea that these seeds would behave as if fully afterripened once the seed zone dropped to near-freezing temperatures. Our simple modification was to let the seeds lose dormancy linearly through the fall, in spite of temperatures below the base for afterripening. This also had the effect of slightly over-accelerating earlier fractions. A more sophisticated TAR model based on an incubation temperature range that includes near-freezing temperatures would have enabled us to model the autumn germination response of the Potosi Pass population with more precision.

Finch-Savage *et al.* (2005, and references cited therein) summarized and discussed a number of possible sources of error associated with hydrothermal modelling under field conditions that we did not specifically address in our study, including seed–soil contact (i.e. which could alter liquid and vapour-phase water uptake and loss during imbibition and drying), hysteresis associated with matric potential that would result in a different soil moisture release curve depending on whether soil was drying or wetting, and changes in seed zone conditions through time. These factors can contribute to differences between water potential of the seeds and the soil. However, all these possibilities are minimized in our study because sensors were located in nearly the identical soil environment as that experienced by the seeds.

One reason our model generally performed well was that we were able to measure seed zone water potential directly. Capacitance sensors have several advantages over more traditional sensors in this regard (e.g. gypsum blocks, Roundy *et al.*, 2007). Capacitance sensors measure a narrow, defined increment of soil depth, equilibrate very rapidly, measure water content accurately over a wide range, and can be placed very close to the surface. Unlike time domain reflectrometry sensors, they have a simple voltage as output and can be wired directly to most data loggers. Careful external calibration using the soil from the field site is necessary, but once this has been performed, the sensors provide output that requires very little manipulation to make it usable for simulation modelling.

Another approach to simulation of field germination phenology utilizes water potential limit models, which allow thermal time accumulation equivalent to accumulation in free water at any water potential above a base. These models can sometimes fit field emergence data as well or better than strict HTT models, possibly because they are not so reliant on precise seed zone water potential information (e.g. Finch-Savage *et al.*, 2005). Because of the short time periods that seeds spend at intermediate water potentials, germination predictions based on water potential limit models may often be as robust as those based on strict HTT (Roundy *et al.*, 2007).

To extend our predictive HTT model for field germination phenology to have broader application would require modifications to the approach described here. At this stage, the model is useful only for seeds that lose dormancy through dry afterripening, but modifications could be made based on thermal time models for other types of dormancy loss, for example, through cold stratification (Steadman and Pritchard, 2004; Allen *et al.*, 2007). Addition of a seedling growth and emergence module would make it possible to predict seedling emergence, which is more readily observed, rather than germination *per se* (Forcella *et al.*, 2000; Taylor *et al.*, 2007). The conceptual simplicity of the HTT approach to predictive seed germination modelling also makes it a logical starting point for examination of more complex patterns of seed dormancy loss and acquisition.

Acknowledgements

The data collection phase of this research was funded through Grant Number 93-38300-8688 from the USDA CSREES Rangelands Special Grants Program.

References

Allen, P.S., White, D.B. and Markhart, A.H. (1993) Germination of perennial ryegrass and annual bluegrass seeds subjected to hydration–dehydration cycles. *Crop Science* **33**, 1020–1025.

Allen, P.S., Debaene-Gill, S. and Meyer, S.E. (1994) Regulation of germination timing in facultatively fall-emerging grasses. pp. 215–219 *in* Monsen, S.B.; Kitchen, S.G. (Eds) *Symposium on Ecology, Management, and Restoration of Intermountain Annual Rangelands, Boise, Idaho, May 18–22, 1992*. Ogden, UT, USDA, Forest Service, Intermountain Research Station, Gen. Tech. Rep. INT-GTR-313.

Allen, P.S., Benech-Arnold, R.L., Batlla, D. and Bradford, K.J. (2007) Modeling of seed dormancy. pp. 72–112 *in* Bradford, K.J.; Nonogaki, H. (Eds) *Seed development, dormancy, and germinaton*. Oxford, UK, Blackwell Publishing.

Alvarado, V. and Bradford, K.J. (2002) A hydrothermal time model explains the cardinal temperatures for seed germination. *Plant, Cell and Environment* **25**, 1061–1069.

Bair, N.B., Meyer, S.E. and Allen, P.S. (2006) A hydrothermal after-ripening time model for seed dormancy loss in *Bromus tectorum* L. *Seed Science Research* **16**, 17–28.

Bauer, M.C., Meyer, S.E. and Allen, P.S. (1998) A simulation model to predict seed dormancy loss in the field for *Bromus tectorum* L. *Journal of Experimental Botany* **49**, 1235–1244.

Bewley, D.J. and Black, M. (1994) *Seeds: physiology of development and germination* (2nd edition). New York, Plenum Press.

Bradford, K.J. (1990) A water relations analysis of seed germination rates. *Plant Physiology* **94**, 840–849.

Bradford, K.J. (1995) Water relations in seed germination. pp. 351–396 *in* Kigel, J.; Galili, G. (Eds) *Seed development and germination*. New York, Marcel Dekker Inc.

Bradford, K.J. and Haigh, A.M. (1994) Relationship between accumulated hydrothermal time during priming and subsequent seed germination rates. *Seed Science Research* **4**, 1–10.

Bradford, K.J., Côme, D. and Corbineau, F. (2007) Quantifying the oxygen sensitivity of seed germination using a population-based threshold model. *Seed Science Research* **17**, 33–43.

Cheng, Z. and Bradford, K.J. (1999) Hydrothermal time analysis of tomato seed germination responses to priming treatments. *Journal of Experimental Botany* **50**, 89–99.

Christensen, M., Meyer, S.E. and Allen, P.S. (1996) A hydrothermal time model of seed after-ripening in *Bromus tectorum* L. *Seed Science Research* **6**, 155–163.

Debaene, S.B.G., Allen, P.S. and White, D.B. (1994) Dehydration of germinating perennial ryegrass seeds can alter rate of subsequent radicle emergence. *Journal of Experimental Botany* **45**, 1301–1307.

Dutta, S. and Bradford, K.J. (1994) Water relations of lettuce seed thermoinhibition. II. Ethylene and endosperm effects on base water potential. *Seed Science Research* **4**, 11–18.

Finch-Savage, W.E., Rowse, H.R. and Dent, K.C. (2005) Development of combined imbibition and hydrothermal threshold models to simulate maize (*Zea mays*) and chickpea (*Cicer arientinum*) seed germination in variable environments. *New Phytologist* **165**, 825–838.

Forcella, F. (1998) Real-time assessment of seed dormancy and seedling growth for weed management. *Seed Science Research* **8**, 201–209.

Forcella, F., Benech-Arnold, R.L., Sanchez, R.A. and Ghersa, C.M. (2000) Modeling seedling emergence. *Field Crops Research* **67**, 123–139.

Gianinetti, A. and Cohn, M.A. (2007) Seed dormancy in red rice. XII. Population-based analysis of dry-afterripening with a hydrotime model. *Seed Science Research* **17**, 253–271.

Gummerson, R.J. (1986) The effect of constant temperatures and osmotic potentials on the germination of sugar beet. *Journal of Experimental Botany* **37**, 729–741.

Hanks, R.J. (1992) *Applied soil physics*. New York, Springer-Verlag.

Kebreab, E. and Murdoch, A.J. (1999) Modeling the effects of water stress and temperature on germination rate of *Orobanche aegyptica* seeds. *Journal of Experimental Botany* **50**, 655–664.

Meyer, S.E. and Allen, P.S. (1999) Ecological genetics of seed germination regulation in *Bromus tectorum* L. I. Phenotypic variance among and within populations. *Oecologia* **120**, 27–34.

Meyer, S.E., Debaene-Gill, S.B. and Allen, P.S. (2000) Using hydrothermal time concepts to model seed germination response to temperature, dormancy loss, and priming effects in *Elymus elymoides*. *Seed Science Research* **10**, 213–223.

Ni, B. and Bradford, K.J. (1992) Quantitative models characterizing seed germination responses to abscisic acid and osmoticum. *Plant Physiology* **98**, 1057–1068.

Roundy, B.A., Hardegree, S.P., Chambers, J.C. and Whittaker, A. (2007) Prediction of cheatgrass field germination potential using wet thermal accumulation. *Rangeland Ecology and Management* **60**, 613–623.

Rowse, H.R. and Finch-Savage, W.E. (2003) Hydrothermal threshold models can describe the germination response of carrot (*Daucus carota*) and onion (*Allium cepa*) seed populations across both sub- and supra-optimal temperatures. *New Phytologist* **158**, 101–108.

Steadman, K.J. and Pritchard, H.W. (2004) Germination of *Aesculus hippocastanum* seeds following cold-induced dormancy loss can be described in relation to a temperature-dependent reduction in base temperature (b) and thermal time. *New Phytologist* **161**, 415–425.

Taylor, J.R., Roundy, B.A., Allen, P.S., Meyer, S.E. and Eggett, D.L. (2007) Soil water sensor accuracy for predicting seedling emergence using a hydrothermal time model. *Arid Land Research and Management* **21**, 229–243.

Vleeshouwers, L.M. and Bouwmeester, H.J. (2001) A simulation model for seasonal changes in dormancy and germination of seeds. *Seed Science Research* **11**, 135–148.